JOURNAL OF GUIDANCE, CONTROL, AND DYNAMICS
Vol. 32, No. 4, July–August 2009

Immersion- and Invariance-Based Adaptive Control of a Nonlinear Aeroelastic System

Keum W. Lee*
University of Kwandong, Gangwon 210-701, Republic of Korea
and
Sahjendra N. Singh†
University of Nevada, Las Vegas, Las Vegas, Nevada 89154-4026

DOI: 10.2514/1.42475

This paper treats the question of adaptive control of prototypical aeroelastic wing sections with structural nonlinearity based on the immersion and invariance approach. The chosen dynamic model describes the nonlinear plunge and pitch motion of a wing. A single control surface is used for the purpose of control. It is assumed that the model parameters except the sign of coefficient of control input are unknown. A noncertainty-equivalent adaptive control law for the trajectory tracking of the pitch angle is derived. Using Lyapunov analysis, asymptotic convergence of the state variables to the origin is established. Unlike the certainty-equivalent control laws developed in literature for aeroelastic systems, this new control system can accomplish superior tracking performance. A special feature of the designed control system is that, whenever the estimated parameters coincide with their true values, the adaptation stops and the closed-loop system recovers the performance of deterministic closed-loop system. This cannot happen if certainty-equivalent adaptive controllers are used. Furthermore, the trajectory of the closed-loop system, including the noncertainty-equivalent adaptive law, is eventually confined to a manifold in the space of state variables and parameter estimates. Simulation results using the new controller and the conventional certainty-equivalent controller are presented. These results show that the new controller performs better in suppressing oscillatory responses of the wing in the presence of large parameter uncertainties.

Nomenclature

a	=	nondimensionalized distance from the midchord to the elastic axis
b	=	semichord of the wing
c_h	=	structural damping coefficient in plunge due to viscous damping
c_α	=	structural damping coefficient in pitch due to viscous damping
c_1, Γ	=	control gain and weighting matrix
h	=	plunge displacement
I_α	=	mass moment of inertia of the wing about the elastic axis
k_h	=	structural spring constant in plunge
k_α	=	structural spring constant in pitch
M, g_0, b_0	=	system matrices
m_t	=	mass of the plunge–pitch system
m_w	=	mass of the wing
s_p	=	span
U	=	freestream velocity
V_i, V	=	Lyapunov functions
x	=	states
x_α	=	nondimensionalized distance measured from the elastic axis to the center of mass
z_i	=	parameter errors
α	=	pitch angle
α_r	=	pitch angle reference trajectory
β	=	flap deflection
γ_i	=	parameter used in update law
θ_i	=	partial parameter estimates
μ_i, μ	=	nonlinear function used in parameter error expression
ρ	=	density of air

Received 30 November 2008; revision received 13 April 2009; accepted for publication 13 April 2009.

*Professor, Division of Electronic Information and Communication Engineering.

†Professor, Department of Electrical and Computer Engineering. Associate Fellow AIAA.

I. Introduction

AEROELASTIC systems exhibit a variety of phenomena including instability, limit cycle, and even chaotic vibration [1,2]. Researchers in aerodynamics, structures, materials, and control have made interesting contributions to the analysis and control of aeroelastic systems. In a recent article, an excellent historical perspective on analysis and control of aeroelastic systems has been provided by Mukhopadhyay [3]. For stability analysis of uncertain aeroelastic models, authors have used the μ method [4]. At the NASA Langley Research Center, a benchmark active control technology (BACT) wind-tunnel model has been designed and control algorithms for flutter suppression have been developed [5–9]. Scott et al. [6] and Bennett et al. [7] describe unsteady aerodynamic data for the BACT project model. The classical and minmax methods have been used to derive robust flutter control systems [8]. Robust passification techniques have been used in [9] for control. Gain scheduled controllers have been designed in [10]. Neural and adaptive control of transonic wind-tunnel model have been considered [11,12]. A 2-degrees-of-freedom aeroelastic model has been developed and tests have been performed in a wind tunnel to examine the effect of nonlinear structural stiffness, and control systems have been designed using linear control theory and the feedback linearizing technique [13–15].

For large parameter uncertainties, a variety of robust, direct, and indirect adaptive controllers for the aeroelastic model of [13] have been developed [16–20]. In the direct adaptive controllers, the gains of the controller are directly tuned. Indirect adaptive systems have a modular structure including a stabilizer and a parameter identifier

[20]. These adaptive laws have been designed based on the certainty-equivalence principle. The controller of these adaptive systems is capable of stabilizing the plant when all the system parameters are known. In certainty-equivalent adaptive (CEA) controllers, the estimated parameters of the controller or the plant are used for the synthesis of controllers. Recently, using the immersion and invariance theory for nonlinear systems, noncertainty-equivalent adaptive (NCEA) control systems have been developed [21–23]. In this design, the estimates produced by the adaptation law provide only the partial estimate of true parameters. For the synthesis of the controller, the full estimate of parameters is obtained by combining these partial estimates with nonlinear functions of states. This is an important difference between this controller and the certainty-equivalent adaptive controllers. Interestingly, whenever the estimation error is zero, adaptation stops, and the closed-loop system recovers the performance of the control system designed for known parameters. Unlike this, in the designs based on the certainty-equivalence principle, adaptation never stops even when the estimated parameters are set to the true values. A noncertainty-based adaptive law has been developed for the attitude control of a rigid body and its superior performance compared to conventional adaptive laws has been demonstrated [24]. It appears from literature, despite this, noncertainty-equivalent adaptive controllers have not been designed for aeroelastic systems. As such, it is of interest to explore the applicability of the new design technique for control of aeroelastic systems.

In this paper, we explore the design of a noncertainty-equivalent adaptive control system for the control of an aeroelastic system. The chosen aeroelastic model [13,14] describes the nonlinear plunge and pitch motion of a wing. This type of model has traditionally been used for the theoretical as well as experimental analysis of two-dimensional aeroelastic behavior. The model has pitch polynomial-type structural nonlinearities. It is assumed that all the system parameters are unknown to the designer, but the sign of control effectiveness coefficient is known. The aeroelastic model has quasi-steady aerodynamic linear aerodynamics, however, it is noted that one can extend this approach to the case of nonlinear aerodynamics as well. This aeroelastic model exhibits undesirable limit cycle oscillations (LCOs) for a set of values of the freestream velocity and the distance of the elastic axis from the midchord. It is essential to minimize or, preferably, completely suppress these oscillations. For the control of this oscillatory behavior, an adaptive control system is designed by treating the pitch angle as a controlled output variable. An update law is derived to provide a partial estimate of the controller parameters. These are combined with nonlinear functions of the state variables to obtain a full estimate of stabilizing gains for the synthesis of the adaptive controller. The closed-loop system can be represented as a cascaded interconnection of two stable subsystems for which the stabilizing and adaptation gains can be tuned independently. This modularity property is similar to the certainty-equivalent indirect adaptive control system for the aeroelastic model of [20], but here modification of the adaptation law using a projection operator is not required to avoid singularity in the control law. It is shown that, in the closed-loop system, the pitch angle trajectory converges to the reference trajectory and oscillations in the state variables are suppressed. For the purpose of comparison, the conventional certainty-equivalent control law is also presented. The NCEA control law has some interesting features. Unlike the CEA design, the manifold in the space of state variables and partial parameter estimates on which the parameter estimation error is zero, is indeed an invariant manifold. As such, if the parameter error becomes zero during the adaptation process, it remains zero thereafter. Moreover, there exists a manifold to which the closed-loop trajectories are attracted. Simulation results for the control of oscillatory motion of the aeroelastic system for various flow velocities and elastic axis locations using the NCEA law and CEA law are presented. It is seen that the NCEA law can give superior performance compared to the CEA law, in spite of large parameter uncertainties.

The organization of the paper is as follows. Section II presents the aeroelastic model. An noncertainty-equivalent adaptive law for the pitch angle control is derived in Sec. III. A certainty-equivalent law is derived in Sec. IV. Finally, Sec. V presents the simulation results.

II. Aeroelastic Model and Control Problem

The prototypical aeroelastic wing section is shown in Fig. 1. A laboratory model of this has been developed at Texas A&M University. The governing equations of motion are provided in [13], which are given by

$$\begin{bmatrix} m_t & m_w x_\alpha b \\ m_w x_\alpha b & I_\alpha \end{bmatrix}\begin{bmatrix} \ddot{h} \\ \ddot{\alpha} \end{bmatrix} + \begin{bmatrix} c_h & 0 \\ 0 & c_\alpha \end{bmatrix}\begin{bmatrix} \dot{h} \\ \dot{\alpha} \end{bmatrix} + \begin{bmatrix} k_{h0} & 0 \\ 0 & k_\alpha(\alpha) \end{bmatrix}\begin{bmatrix} h \\ \alpha \end{bmatrix} = \begin{bmatrix} -L \\ M \end{bmatrix} \tag{1}$$

where h is the plunge displacement and α is the pitch angle. In Eq. (1), m_w is the mass of the wing, m_t is the total mass, b is the semichord of the wing, I_α is the moment of inertia, x_α is the nondimensionalized distance of the center of mass from the elastic axis, c_α and c_h are the pitch and plunge damping coefficients, respectively, and M and L are the aerodynamic moment and lift. It is assumed that the quasi-steady aerodynamic force and moment are of the form

$$L = \rho U^2 b c_{l_\alpha} s_p \left[\alpha + \frac{\dot{h}}{U} + \left(\frac{1}{2} - a\right) b \frac{\dot{\alpha}}{U}\right] + \rho U^2 b c_{l_\beta} s_p \beta$$

$$M = \rho U^2 b^2 c_{m_\alpha} s_p \left[\alpha + \frac{\dot{h}}{U} + \left(\frac{1}{2} - a\right) b \frac{\dot{\alpha}}{U}\right] + \rho U^2 b^2 c_{m_\beta} s_p \beta \tag{2}$$

where a is the nondimensionalized distance from the midchord to the elastic axis, s_p is the span, c_{l_α} and c_{m_α} are the lift and moment coefficients per angle of attack, and c_{l_β} and c_{m_β} are lift and moment coefficients per control surface deflection β. Although other forms of nonlinear spring stiffness associated with the pitch can be considered, for purposes of illustration, the function $k_\alpha(\alpha)$ is considered as a polynomial nonlinearity of fourth degree. This is given by

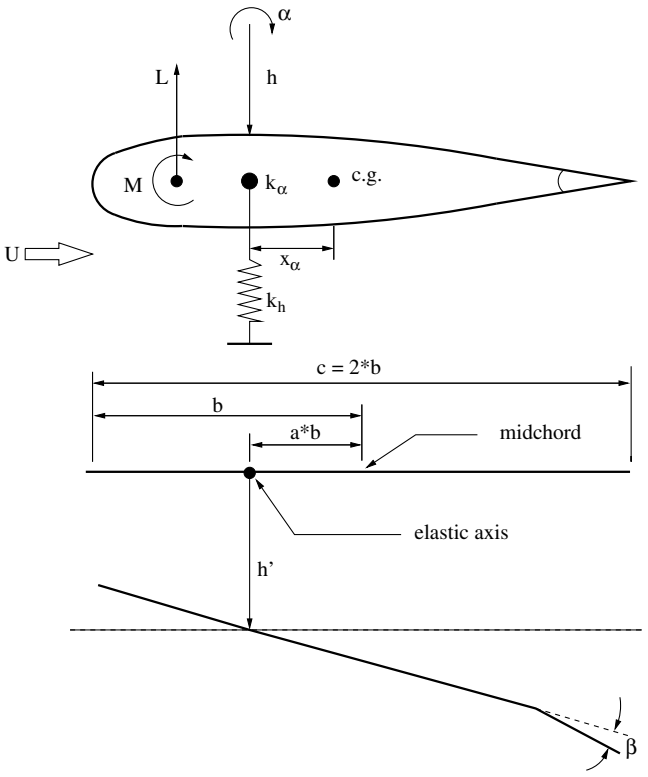

Fig. 1 Aeroelastic model.

$$k_\alpha(\alpha) = k_{\alpha_0} + k_{\alpha_1}\alpha + k_{\alpha_2}\alpha^2 + k_{\alpha_3}\alpha^3 + k_{\alpha_4}\alpha^4$$

Defining the state vector $x = (x_1, \ldots, x_4)^T = (\alpha, h, \dot{\alpha}, \dot{h})^T \in R^4$, one obtains a state variable representation of Eq. (1) in the form

$$\dot{x} = \begin{bmatrix} 0_{2\times 2} & I_{2\times 2} \\ M_s & M_d \end{bmatrix} x + \begin{bmatrix} 0_{2\times 2} \\ g_0 \end{bmatrix} k_{n_\alpha} + \begin{bmatrix} 0_{2\times 1} \\ b_0 \end{bmatrix} \beta \doteq f(x) + B_0\beta \quad (3)$$

where $f(x)$ and B_0 are defined in Eq. (3), $\alpha k_\alpha = \alpha k_{\alpha_0} + k_{n_\alpha}$, $k_{n_\alpha} = \alpha(k_{\alpha_1}\alpha + k_{\alpha_2}\alpha^2 + k_{\alpha_3}\alpha^3 + k_{\alpha_4}\alpha^4)$, k_{ij} are constants, $g_0 = (g_{0i})$ is a 2×1 constant vector, $b_0 = (b_{01}, b_{02})^T$ (T denotes transposition), 0 and I denote null and identity matrices of indicated dimensions, and the matrices $M_a = (M_s, M_d) \in R^{2\times 4}$, g_0, and b_0 are easily obtained from Eq. (1). Let $y = x_1 = \alpha$ be the controlled output variable.

Assumption 1: It is assumed that elements of M_a, g_0, b_0, and k_{α_j} associated with the structural nonlinearity are not known, but the sign of b_{01} is known.

Let α_r be a smooth pitch angle reference trajectory converging to zero. We are interested in the design of a noncertainty-equivalent adaptive controller for the pitch angle trajectory tracking of the reference trajectory and stabilization of the system Eq. (3) under Assumption 1. We assume that the state vector x and the plunge acceleration are measured for feedback. For the laboratory model of the aeroelastic system developed at Texas A&M University, optical encoders are mounted on the plunge and pitch cams to measure plunge and pitch positions. Also, it is equipped with plunge and pitch accelerometers for measuring accelerations. These measurements can be used to compute the state variables. It will be seen that use of acceleration feedback simplifies the design of the control system.

III. Noncertainty-Equivalent Adaptive Control System

In this section, an adaptive control law is designed for the choice of the pitch angle as an output based on an immersion and invariance approach described in [21–23].

First, we note that $f_3(x)$ [$f_i(x)$ is the ith component of vector $f(x)$] can be written in a linearly parameterized form as

$$f_3(x) = \phi^T(x)\theta_1 \quad (4)$$

where

$$\phi(x) = (\alpha, h, \dot{\alpha}, \dot{h}, \alpha^2, \alpha^3, \alpha^4, \alpha^5)^T \in R^8$$

and $\theta_1 \in R^8$ is the vector of unknown parameters. Let

$$\beta = \text{sgn}\,(b_{01})u$$

where u is a new control input. Define $b_1 = b_{01}\,\text{sgn}\,(b_{01}) > 0$. Then, the equation for the pitch acceleration takes the form

$$\ddot{\alpha} = \phi^T(x)\theta_1 + b_1 u \quad (5)$$

The controller consists of an estimator and a control module (stabilizer). First, the design of the control module is considered.

A. Design of Control Module

For controller design, consider a function s_1 which is a linear function of the tracking error $\tilde{\alpha} = \alpha - \alpha_r$ and its derivative given by

$$s_1 = \dot{\tilde{\alpha}} + \lambda\tilde{\alpha} \quad (6)$$

where $\lambda > 0$. In view of Eq. (6), we observe that, if s_1 is zero, then the tracking error tends to zero. As such, it is sufficient to design a controller which forces s_1 to zero.

Because the system parameters are not known, we will need their estimates for the design of control system. Let $\hat{\theta}_1 + \mu_1$ and $\hat{\theta}_2 + \mu_2$ be the estimates of θ_1 and $\theta_2 = b_1^{-1}$ (the inverse of b_1), respectively. In general, μ_i are nonlinear functions of the state x, α_r and its derivatives, and $\hat{\theta}_i$. (Explicit dependence of μ_i on these variables can be seen later.) We can think of $\hat{\theta}_i$ ($i = 1, 2$) as only partial estimates of the actual parameter vector θ_1 and θ_2.

Define the parameter errors as

$$z_1 = \hat{\theta}_1 + \mu_1 - \theta_1 \in R^8 \qquad z_2 = \hat{\theta}_2 + \mu_2 - \theta_2 \in R$$

and define $z = (z_1^T, z_2)^T \in R^9$, $\hat{\theta} = (\hat{\theta}_1^T, \hat{\theta}_2)^T \in R^9$, $\mu = (\mu_1^T, \mu_2)^T \in R^9$, and $\theta = (\theta_1^T, \theta_2)^T \in R^9$.

The derivative of s_1 along the solution of Eq. (5) is given by

$$\dot{s}_1 = \phi^T(x)\theta_1 + \theta_2 u - \ddot{\alpha}_r + \lambda\dot{\tilde{\alpha}} \quad (7)$$

Consider a control input of the form

$$u = (\hat{\theta}_2 + \mu_2)v \quad (8)$$

where v is a new input yet to be determined. Noting that

$$b_1 u = b_1(\hat{\theta}_2 + \mu_2)v = b_1(z_2 + b_1^{-1})v = v + b_1 z_2 v$$

Eq. (7) gives

$$\dot{s}_1 = \phi^T(x)\theta_1 + v + b_1 z_2 v - \ddot{\alpha}_r + \lambda\dot{\tilde{\alpha}} \quad (9)$$

Now, select the control input v to cancel the known and estimated terms as

$$v(x, \hat{\theta}_1, \mu_1, t) = -[\phi^T(x)(\hat{\theta}_1 + \mu_1) + c_1 s_1 - \ddot{\alpha}_r + \lambda\dot{\tilde{\alpha}}] \quad (10)$$

where $c_1 > 0$, and the argument t of v indicates the dependence of v on α_r and its derivatives. Using the control law Eq. (10) in Eq. (9) gives

$$\dot{s}_1 = -\phi^T(x)z_1 - c_1 s_1 + b_1 z_2 v \doteq -c_1 s_1 - \Psi^T(x, \hat{\theta}_1, \mu_1, t)z \quad (11)$$

where

$$\Psi^T(x, \hat{\theta}_1, \mu_1, t) = [\phi^T(x), -b_1 v] \in R^9$$

is a row vector.

For stability analysis, consider a Lyapunov function $V_1(s_1) = s_1^2$. Differentiating s_1 and using Eq. (11) gives

$$\dot{V}_1 = -2c_1 s_1^2 - 2s_1\Psi^T z \quad (12)$$

Using Young's inequality, one has $-2s_1\Psi^T z \le c_1 s_1^2 + c_1^{-1}(\Psi^T z)^2$, which can be substituted in Eq. (12) to yield

$$\dot{V}_1 \le -c_1 s_1^2 + c_1^{-1}(\Psi^T z)^2 \quad (13)$$

We observe from Eq. (13) that if $\Psi^T z$ is bounded then s_1 will be uniformly ultimately bounded. Then, in view of the definition of s_1, it will imply boundedness of the tracking error. The z-dependent term in the derivative of V_1 will be compensated by designing an appropriate estimator.

B. Estimator Design

Now, an estimator is designed such that the parameter error vector z has a desirable property. Using $b_1 u = (1 + b_1 z_2)v$ in Eq. (5) gives

$$\ddot{\alpha} = \phi_1^T(x)\theta_1 + v + b_1 z_2 v \quad (14)$$

The nonlinear vector function μ is a function of x, $\hat{\theta}$, and t. Differentiating $z(x, \hat{\theta}, t)$ gives the dynamics of the parameter error vector as

$$\dot{z} = \dot{\hat{\theta}} + \frac{\partial\mu}{\partial\hat{\theta}}\dot{\hat{\theta}} + \frac{\partial\mu}{\partial\alpha}\dot{\alpha} + \frac{\partial\mu}{\partial h}\dot{h} + \frac{\partial\mu}{\partial\dot{\alpha}}[\phi_1^T(x)\theta_1 + v + b_1 z_2 v] + \frac{\partial\mu}{\partial\dot{h}}\ddot{h} + \frac{\partial\mu}{\partial t} \quad (15)$$

where $(\partial\mu/\partial t)$ denotes the terms arising from the dependence of μ on the reference trajectory and its derivatives. Note that $\ddot{h}$ is available for feedback and it is treated as a known function in Eq. (15).

Now, the update law for $\hat{\theta}$ is selected to cancel known and estimated terms of Eq. (15). It is easily seen that this update law is of the form

$$\dot{\hat{\theta}} = -\left(I_{9\times 9} + \frac{\partial \mu}{\partial \hat{\theta}}\right)^{-1}\left[\frac{\partial \mu}{\partial \alpha}\dot{\alpha} + \frac{\partial \mu}{\partial h}\dot{h} + \frac{\partial \mu}{\partial \dot{\alpha}}[\phi_1^T(x)(\hat{\theta}_1 + \mu_1) + v] + \frac{\partial \mu}{\partial \dot{h}}\ddot{h} + \frac{\partial \mu}{\partial t}\right] \tag{16}$$

Substituting Eq. (16) in Eq. (15) gives

$$\dot{z} = -\frac{\partial \mu}{\partial \dot{\alpha}}[\phi^T(x)z_1 - b_1 z_2 v] \tag{17}$$

Now, the vector function μ must be chosen such that the dynamics of the parameter error vector z has stable behavior. In view of Eq. (17), we choose

$$\frac{\partial \mu_1}{\partial \dot{\alpha}} = \gamma_1 \phi(x) \qquad \frac{\partial \mu_2}{\partial \dot{\alpha}} = -\gamma_2 v(x, \hat{\theta}_1, \mu_1, t) \tag{18}$$

where $\gamma_i > 0$. To obtain μ, one must integrate Eq. (18) with respect to $\dot{\alpha}$. We point out that we have simplified the computation of μ by assuming that $\ddot{h}$ is measured. It can be seen that, if the plunge acceleration is not measured, then the preceding equations will involve the partial derivatives $(\partial \mu_i/\partial \dot{\alpha})$ and $(\partial \mu_i/\partial \dot{h})$, which cause difficulty in finding a proper solution for μ.

Solving for μ_1 from Eq. (18) gives

$$\mu_1(x) = \gamma_1 \int_0^{\dot{\alpha}} \phi(x_1, x_2, \xi, x_4)\, \mathrm{d}\xi = \gamma_1[\alpha, h, 0.5\dot{\alpha}, \dot{h}, \alpha^2, \alpha^3, \alpha^4, \alpha^5]^T\dot{\alpha} \in R^8 \tag{19}$$

Now, $\mu_1(x)$ can be substituted in Eq. (10) to obtain an explicit expression for $v(x, \hat{\theta}_1, t)$. Using the function v, one integrates the second equation of Eq. (18) to obtain μ_2 given by

$$\mu_2(x, \hat{\theta}_1, t) = -\gamma_2 \int_0^{\dot{\alpha}} v(x_1, x_2, \xi, x_4, \hat{\theta}_1, t)\, \mathrm{d}\xi \tag{20}$$

The expression for function μ_2 is given in the Appendix. Now that the nonlinear function μ has been computed, various partial derivatives of μ with respect to x_i, t, and $\hat{\theta}_i$ can be derived and substituted in Eq. (16) to obtain the update law. (These partial derivatives are collected in the Appendix.) It may be pointed out that the matrix $[I_{9\times 9} + (\partial \mu/\partial \hat{\theta})]$ is always nonsingular, and the update law Eq. (16) is well defined for all values of x, $\hat{\theta}$, and t. In fact, one has

$$\frac{\partial \mu}{\partial \hat{\theta}} = \begin{bmatrix} 0_{8\times 8} & 0_{8\times 1} \\ \partial \mu_2/\partial \hat{\theta}_1 & 0 \end{bmatrix}$$

a lower triangular matrix with zero in the diagonal.

Define a positive definite diagonal matrix

$$\Gamma = \mathrm{diag}\{I_{8\times 8}\gamma_1, \gamma_2 b_1^{-1}\}$$

It is noted that, according to Assumption 1, the sign of b_{01} is known. Because $b_1 = b_{01}\,\mathrm{sgn}\,(b_{01}) > 0$, it is possible to select a positive definite matrix Γ despite the lack of knowledge of the value of b_{01}. Then, substituting Eq. (18) in Eq. (17), one obtains the z dynamics in a compact form given by

$$\dot{z} = -\Gamma \Psi(x, \hat{\theta}_1, t)\Psi^T(x, \hat{\theta}_1, t)z \tag{21}$$

To examine the stability property of the error dynamics, consider a positive definite Lyapunov function $V_2(z)$ of variable z

$$V_2(z) = c_1^{-1} z^T \Gamma^{-1} z \tag{22}$$

Differentiating V_2 and using Eq. (21) gives

$$\dot{V}_2 = -2c_1^{-1} z^T \Psi \Psi^T z \le 0 \tag{23}$$

Because the derivative of V_2 is negative semidefinite, $z \in L_\infty[0, \infty)$ (the set of bounded functions) and the origin $z = 0$ is uniformly globally stable. Also, integrating Eq. (23) gives

$$\int_0^\infty (\Psi^T z)^2\, \mathrm{d}t = -V_2[z(\infty)] + V_2[z(0)] \le V_2[z(0)]$$

which implies that $\Psi^T z \in L_2[0, \infty)$ (the set of square integrable functions).

Now, we examine the stability property of the complete system Eq. (3) together with the update law Eq. (16). Since s_1 involves only the pitch angle and its derivative, stability of the zero dynamics is essential for the stability in the closed-loop system. The zero dynamics of the system is the residual dynamics of the model Eq. (3), when α is identically zero. If we choose the coordinates $\eta_1 = b_{02}\alpha_1 - b_{01}h$ and $\eta_2 = \dot{\eta}_1$, then one can show that

$$\dot{\eta} = A_\eta \eta + g_\eta(\alpha, \dot{\alpha}) \tag{24}$$

where A_η is a 2×2 constant matrix, g_η is a nonlinear function of indicated arguments, and $\eta = (\eta_1, \eta_2)^T$.

Assumption 2: We assume that the flow velocity and the elastic axis location are such that the matrix A_η is Hurwitz (i.e., the origin of the zero dynamics is exponentially stable).

For the stability analysis of the closed-loop system, consider the composite Lyapunov function $V = V_1 + V_2$. Differentiating V and using Eqs. (13) and (23), one obtains

$$\dot{V} \le -c_1 s_1^2 - c_1^{-1}[\Psi^T(x, \hat{\theta}_1, t)z]^2 \le 0 \tag{25}$$

Because V is a positive definite function of s_1 and z, and $\dot{V} \le 0$, one finds that s_1 and z are bounded. Of course α and its derivative are bounded if s_1 is bounded. In view of Eq. (24), under Assumption 2, h and $\dot{h}$ are bounded, and therefore x is bounded. Since x and z are bounded, μ and $\hat{\theta}$ are bounded. This implies that all the signals including u are bounded. Because derivatives of s_1 and $\Psi^T z$ are bounded, and s_1 and $\Psi^T z$ are square integrable functions, using Barbalat's lemma (see [23], p. 268), one concludes that s_1 and $\Psi^T z$ tend to zero. Note that the selected reference trajectory converges to zero. This then implies that α and h converge to zero.

We now summarize these results.

Theorem 1: Consider the closed-loop system Eq. (3) including the control law Eqs. (8) and (10) and the adaptation law Eq. (16). Suppose that the zero dynamics have an exponentially stable equilibrium point. Then, in the closed-loop system, tracking error $\tilde{\alpha}$ and x converge to zero and $z = 0$ is uniformly globally stable. Furthermore, $\Psi(x, \hat{\theta}_1, t)^T z$ asymptotically converges to zero.

To this end, we summarize the special features of the derived control law.

Remark 1: According to Eq. (21), the z dynamics can be treated as a linear time-varying system given as

$$\dot{z} = A(t)z \tag{26}$$

where

$$A(t) = -\Gamma \Psi(x(t), \hat{\theta}(t), t)\Psi^T(x(t), \hat{\theta}(t), t)$$

Therefore, its solution is

$$z(t) = \Phi(t, t_0)z(t_0) \tag{27}$$

where Φ is the transition matrix of $A(t)$. In view of Eq. (27), one notes that, if at some instant $z(t_1) = 0$, then $z(t) = 0$ for $t \ge t_1$; that is, the manifold defined by

$$M_z = \{(x, \hat{\theta}) \in R^4 \times R^9 : \hat{\theta} + \mu(x, \hat{\theta}, t) - \theta = 0\}$$

is an invariant manifold. As such, the parameter vector estimate $\hat{\theta} + \mu$ remains frozen at its actual value for $t \ge t_1$. Consequently, the

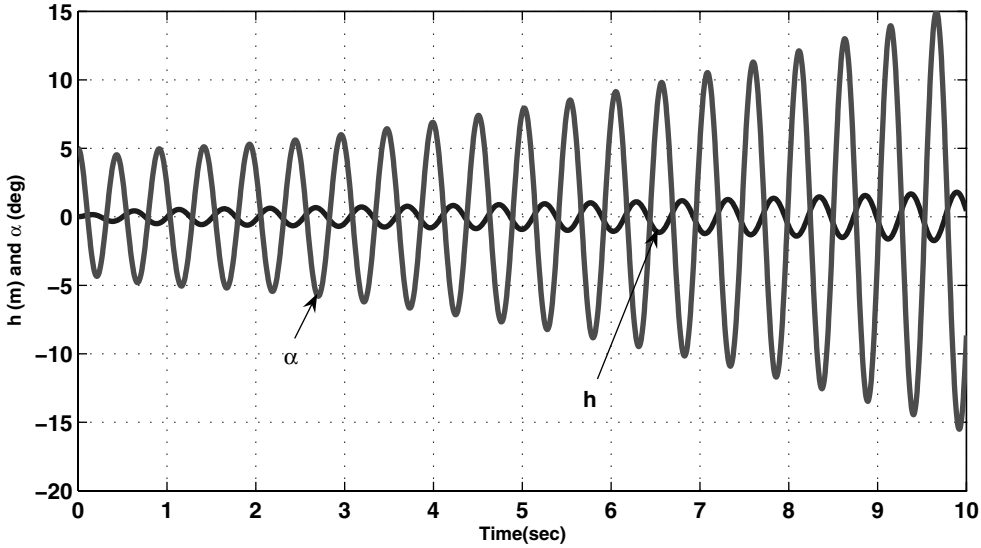

Fig. 2 Open-loop divergent behavior of the linear model: $U = 17$ m/s, $a = -0.6547$.

closed-loop system recovers the performance of the deterministic control law designed for known parameters.

Remark 2: According to Theorem 1, one concludes that the trajectory of the closed-loop system eventually resides in the manifold defined by

$$\Omega = \{(x, \hat{\theta}) \in R^4 \times R^9 : \Psi(x, \hat{\theta}_1)^T [\hat{\theta} + \mu(x, \hat{\theta}) - \theta] = 0 \qquad (28)$$

It is important to note that $\Psi^T z$ will converge to zero even if $\Psi(t = \infty)$ is not zero.

IV. Certainty-Equivalent Control Law

In this section, for the purpose of comparison, a certainty-equivalent adaptive control law is briefly described. We retain the function s_1 for derivation. Let $\hat{\theta}_1$ and $\hat{\theta}_2$ be the estimates of θ_1 and $\theta_2 = b_1^{-1}$; that is, now one takes $\mu_i = 0$ $(i = 1, 2)$. Thus, the parameter estimate errors are $z_1 = \hat{\theta}_1 - \theta_1$ and $z_2 = \hat{\theta}_2 - \theta_2$. The control input u is now

$$u = \hat{\theta}_2 v$$

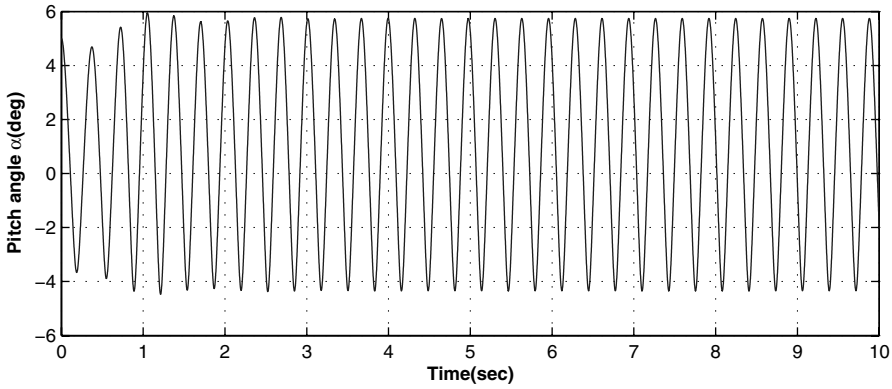

a)

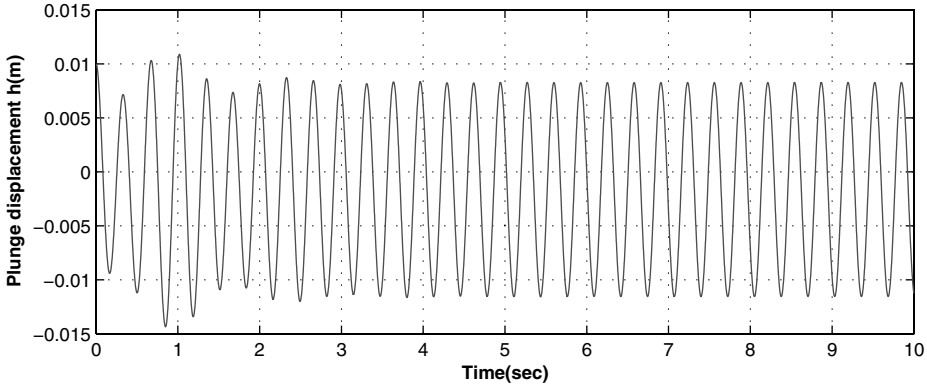

b)

Fig. 3 Open-loop response of the nonlinear model showing LCO; $U = 20$ m/s, $a = -0.6547$: a) pitch angle α, deg, and b) plunge displacement h, m.

where, in view of Eq. (10) with $\mu = 0$, the simplified control law takes the form

$$v = -[\phi^T(x)\hat{\theta}_1 + c_1 s_1 - \ddot{\alpha}_r + \lambda\dot{\tilde{\alpha}}] \tag{29}$$

Substituting the control law in Eq. (9) gives

$$\dot{s}_1 = -c_1 s_1 - \phi^T(x) z_1 + b_1 z_2 v \tag{30}$$

For examining the stability in the closed-loop systems, consider a Lyapunov function

$$W = s_1^2 + \gamma_1^{-1} z_1^T z_1 + b_1 \gamma_2^{-1} z_2^2 \tag{31}$$

Differentiating W gives

$$\dot{W} = 2s_1[-c_1 s_1 - \phi^T(x) z_1 + b_1 z_2 v] + 2\gamma_1^{-1} z_1 \dot{\hat{\theta}}_1 + 2b_1 \gamma_2^{-1} z_2 \dot{\hat{\theta}}_2 \tag{32}$$

Then, it easily follows that, by the choice of the adaptation law,

$$\dot{\hat{\theta}}_1 = \gamma_1 \phi_1(x) s_1 \qquad \dot{\hat{\theta}}_2 = -\gamma_2 v s_1 \tag{33}$$

the Lyapunov derivative simplifies to

$$\dot{W} = -2c_1 s_1^2 \tag{34}$$

In view of Eq. (34), $s_1 \in L_\infty[0, \infty) \bigcap L_2[0, \infty)$ and $\hat{\theta}_i \in L_\infty[0, \infty)$. Now, based on Barbalat's lemma, under Assumption 2, one can show that $\tilde{\alpha}$ and x converge to zero.

Now, we can compare the two adaptive control systems. First, we notice that, unlike Eq. (34), the Lyapunov derivative Eq. (25) for a noncertainty-equivalent controller has an additional nonnegative term, which can cause faster decay of V. One important point to note here is that the adaptation law Eq. (33) for the certainty-equivalent control system is a function of s_1 which depends on the tracking error. As such, the parameter estimates keep on drifting, even if they initially coincide with their actual values, because the tracking error is nonzero. This is unlike the estimator property described in

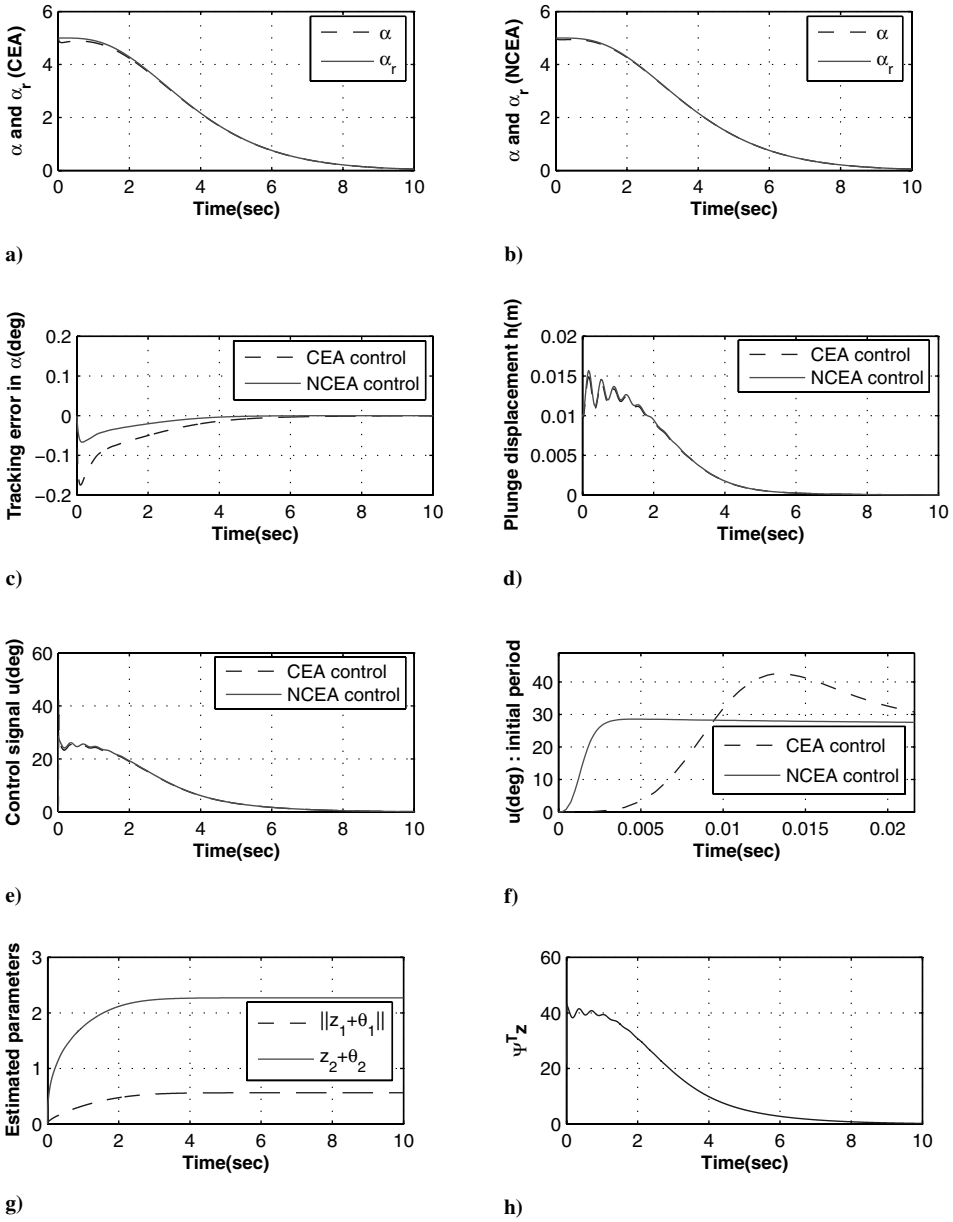

Fig. 4 Closed-loop control; $U = 20$ m/s, $a = -0.6547$: a) pitch angle α (dashed line) and reference angle α_r (solid line) (CEA); b) pitch angle α (dashed line) and reference angle α_r (solid line) (NCEA); c) tracking error of pitch angle α in CEA (dashed line) and NCEA (solid line); d) plunge displacement in CEA (dashed line) and NCEA (solid line); e) control input u in CEA (dashed line) and NCEA (solid line); f) control input u in CEA (dashed line) and NCEA (solid line), initial period; g) estimated parameters for NCEA law [$\|z_1 + \theta_1\|$ (dashed line) and $z_2 + \theta_2$ (solid line)]; h) $\Psi^T z$ for NCEA law.

Remark 1 for the noncertainty-equivalent adaptive design. It is noted that, in this special case of $\alpha_r(\infty) = 0$, Ψ tends to zero. As such, $\Psi^T z$ naturally tends to zero as well. However, unlike the NCEA law, the CEA law cannot guarantee convergence of $\Psi^T z$ to zero, if $\alpha_r(\infty)$ is nonzero.

V. Simulation Results

This section presents the results of digital simulation. The model parameters are taken from [13,14]. The system parameters are collected in the Appendix. Both the NCEA law and the CEA law are simulated. The initial conditions chosen are $h(0) = 0.01$ m, $\alpha(0) = 5$ deg, and $\dot{\alpha}(0) = \dot{h}(0) = 0$. For generating a smooth reference pitch angle trajectory, a fourth-order filter of the form

$$(s^2 + 2\rho_1\omega_1 s + \omega_1^2)(s^2 + 2\rho_2\omega_2 s + \omega_2^2)\alpha_r(t) = 0$$

is used, where s denotes the derivative operator. The filter parameters are $\rho_1 = \rho_2 = 1$, $\omega_1 = \omega_2 = 1$. The derivatives of the command trajectory are set to zero at $t = 0$, but one has $\alpha_r(0) = 5$ deg. The controller parameters are $\lambda = 40$, $c_1 = 40$, and the adaptation parameters are selected as $\gamma_1 = \gamma_2 = 10$. The initial values of the partial estimates are arbitrarily set as $\hat{\theta}_i(0) = 0$ $(i = 0, 1)$. This is a rather worse choice of estimates but is made to evaluate the robustness of the controller. (For the actual values of the parameters θ_1 and θ_2, see the Appendix.) The poles of the linearized system for $U = 20$ m/s and $a = -0.6547$ are $1.1975 \pm 13.0787i$, $-3.3905 \pm 13.5807i$, and the zeros are $-1.6279 \pm 17.5836i$. Thus, the open-loop system is unstable and the linearized system is minimum phase.

First, the behavior of the open-loop linear model without nonlinearity is analyzed. It is found that, for a fixed parameter a, the linear system has stable poles for smaller values of the freestream velocity, and the two branches of the root loci cross the imaginary axis in the complex plane from left-hand side (stable region) to the right-hand side (unstable region) as the velocity increases. The critical speed at which two purely imaginary poles appear is approximately $U = 16.67495$ m/s for $a = -0.6457$. Beyond this critical speed, the linear model is unstable. Figure 2 shows the divergent plunge and pitch motion of the linear model (ignoring

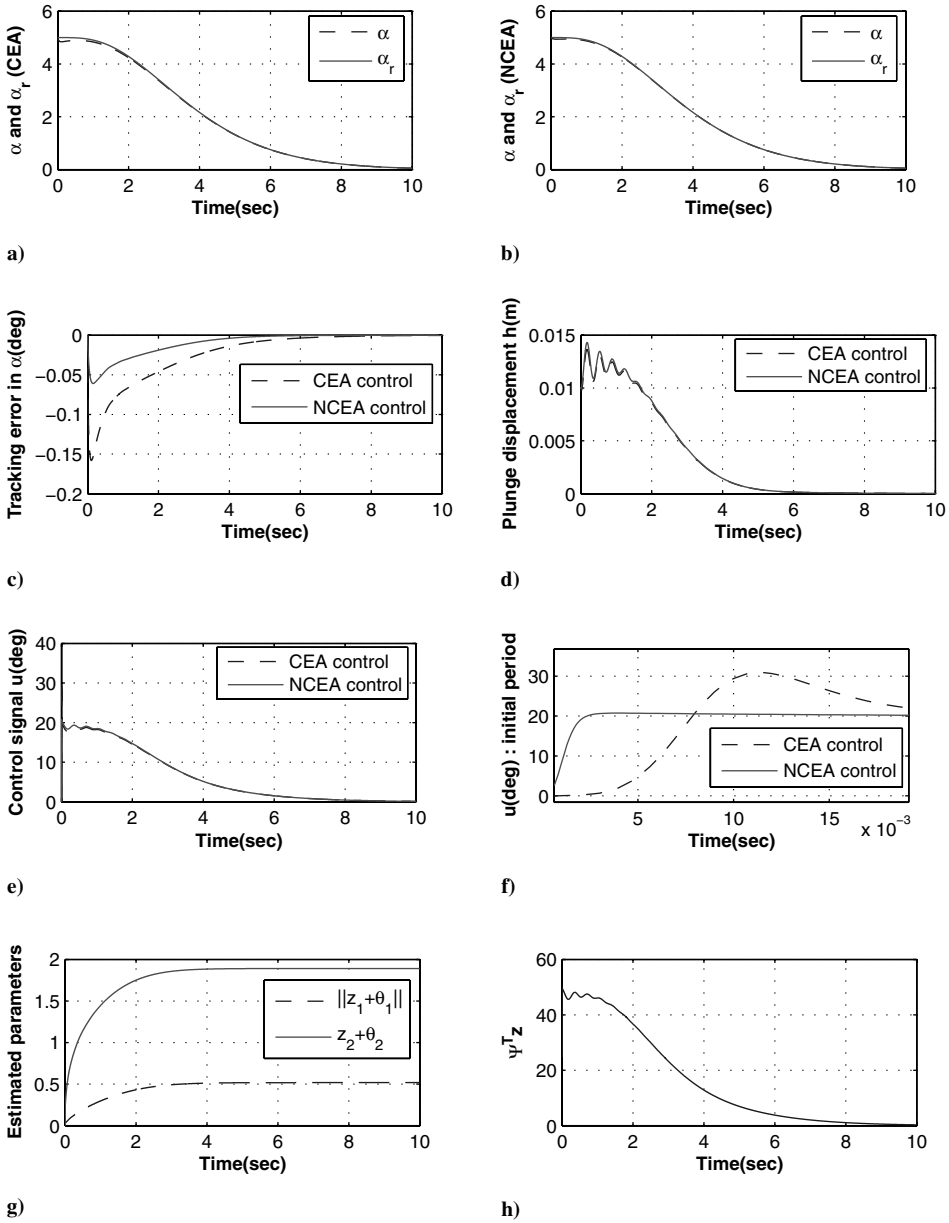

Fig. 5 Closed-loop control; $U = 25$ m/s, $a = -0.6547$: a) pitch angle α (dashed line) and reference angle α_r (solid line) (CEA); b) pitch angle α (dashed line) and reference angle α_r (solid line) (NCEA); c) tracking error of pitch angle α in CEA (dashed line) and NCEA (solid line); d) plunge displacement in CEA (dashed line) and NCEA (solid line); e) control input u in CEA (dashed line) and NCEA (solid line); f) control input u in CEA (dashed line) and NCEA (solid line), initial period; g) estimated parameters for NCEA law [$\|z_1 + \theta_1\|$ (dashed line) and $z_2 + \theta_2$ (solid line)]; h) $\Psi^T z$ for NCEA law.

nonlinear functions) for a value of $U = 17$ m/s. In the open-loop nonlinear model Eq. (1), as the freestream velocity passes through the critical value, the supercritical Andronov–Hopf bifurcation takes place and unique limit cycle bifurcates from the equilibrium point $x = 0$. The amplitude and frequency of oscillation of the limit cycle are functions of the freestream velocity and the parameter a [25].

To show the oscillatory behavior of the open-loop nonlinear model, responses for $U = 20$ m/s and $a = -0.6547$ are obtained. We observe a limit cycle oscillation in the steady state as expected. The oscillatory pitch and plunge responses are shown in Fig. 3. Now, control of oscillatory motion is considered. Both the NCEA law and the CEA law for the model with different values of U and a are simulated. Note that, for the purpose of comparison, the same control gains (c_1, λ) and the adaptation parameters (γ_i) are used for the two control systems.

Case A: Closed-Loop Control $U = 20$ m/s, $a = -0.6547$

The closed-loop systems including the NCEA law and the CEA law for $U = 20$ m/s, $a = -0.6547$ are simulated. The selected responses are shown in Fig. 4. The figure shows that the pitch angle trajectory smoothly converges to α_r, and the state vector converges to the origin. We observe oscillatory plunge displacement response. This is because the zero dynamics have stable but complex conjugate poles. We observe that the NCEA law gives better tracking performance compared to the CEA law, and tracking error with the CEA law is larger in the transient period (Fig. 4c). Interestingly, the NCEA law gives smaller peak value in the control input magnitude (Fig. 4f). We observe that the parameter estimates $\hat{\theta}_i + \mu_i$ ($i = 1, 2$) converge to some constant values, which differ from the actual values. This is not unusual, because convergence of parameters requires satisfaction of certain persistent excitation conditions. Also, the plot of $\Psi^T z$ is given. (In all the figures, the parameter estimates and the function $\Psi^T z$ are plotted only for the NCEA law to save space.) The maximum control surface deflections are 42.5 deg (CEA) and 28.5 deg (NCEA). This is shown in a separate Fig. 4f for clarity.

Case B: Closed-Loop Control $U = 25$ m/s, $a = -0.6547$

To examine the sensitivity of the controller with respect to variation in the freestream velocity, simulation is done for a different

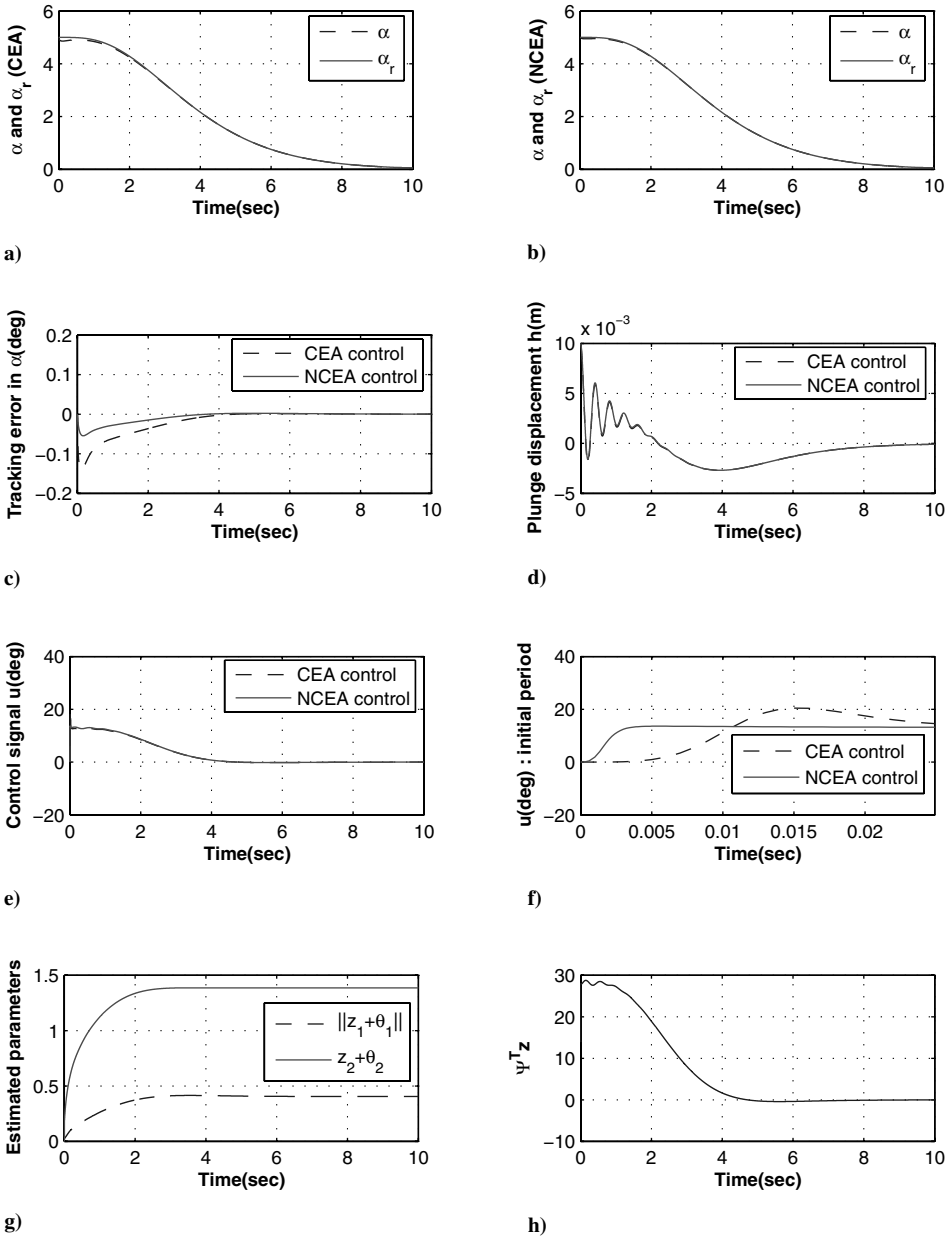

Fig. 6 Closed-loop control; $U = 20$ m/s, $a = -0.4$: a) pitch angle α (dashed line) and reference angle α_r (solid line) (CEA); b) pitch angle α (dashed line) and reference angle α_r (solid line) (NCEA); c) tracking error of pitch angle α in CEA (dashed line) and NCEA (solid line); d) plunge displacement in CEA (dashed line) and NCEA (solid line); e) control input u in CEA (dashed line) and NCEA (solid line); f) control input u in CEA (dashed line) and NCEA (solid line), initial period; g) estimated parameters for NCEA law [$\|z_1 + \theta_1\|$ (dashed line) and $z_2 + \theta_2$ (solid line)]; h) $\Psi^T z$ for NCEA law.

value of $U = 25$ m/s, but the value of a is not changed. The remaining parameters of case A are retained. The responses are shown in Fig. 5. We again observe convergence of the tracking error and the state vector to zero. Similar to case A, the NCEA law gives better performance compared with the CEA law. This is evident from the plot of the tracking error in Fig. 5c and the control input plot in Fig. 5f. We observe a larger tracking error overshoot of about 0.15 with the CEA law compared to nearly 0.05 with the NCEA law (Fig. 5c). The maximum control surface deflections are 30.9 deg (CEA) and 20.7 deg (NCEA). For this case, smaller control magnitude compared to case A is needed because the control input coefficient is larger at higher velocity U.

Case C: Closed-Loop Control $U = 20$ m/s, $a = -0.4$

For examining the robustness with respect to a, responses are obtained for $U = 20$ m/s and $a = -0.4$. The remaining parameters of case A are retained. The selected responses are shown in Fig. 6. We observe suppression of the oscillatory responses. Similar to case A and case B, it is seen that the NCEA law gives better tracking error convergence performance requiring smaller overshoot and smaller control magnitude. The maximum control surface deflections are 20.5 deg (CEA) and 13.6 deg (NCEA). For this value of a, both control laws require smaller control magnitude compared to case A.

Case D: Closed-Loop Control $U = 25$ m/s, $a = -0.4$

Finally, a simulation is presented for $a = -0.4$ at a higher freestream velocity of $U = 25$ m/s. The remaining parameters of case A are retained. The responses in Fig. 7 show suppression of oscillatory motion of the system. As expected, smaller control inputs compared to case C are required. Again, we observe larger peaks in tracking error and control input with the CEA law. The maximum control surface deflections are 10.1 deg (CEA) and 7.1 deg (NCEA).

Extensive simulation has been performed for other values of the freestream velocity and the parameter a. In each case, it has been observed that the NCEA law and the CEA law accomplish control of the oscillatory motion of the aeroelastic system. However, the NCEA law gives better performance compared wtih the CEA law.

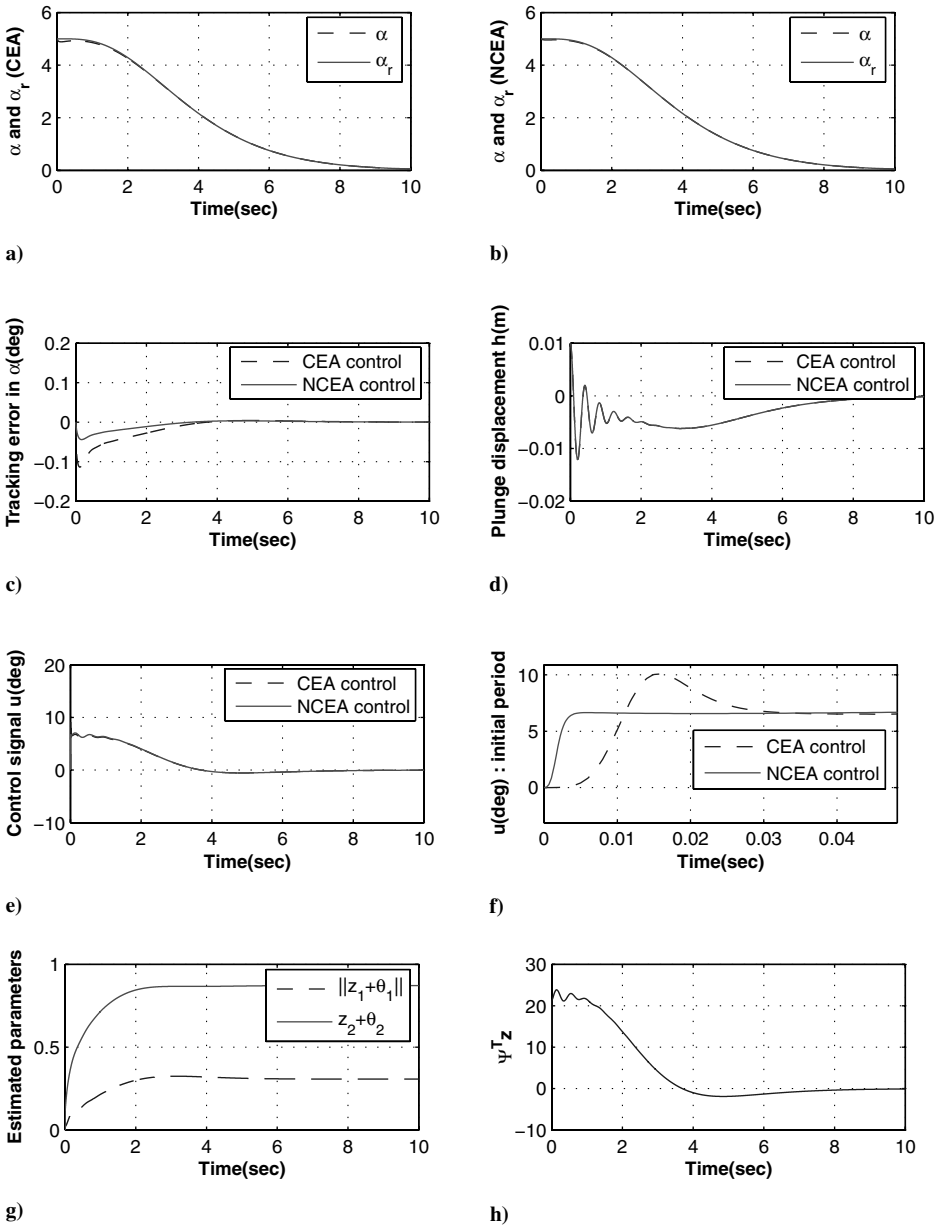

Fig. 7 Closed-loop control; $U = 25$ m/s, $a = -0.4$: a) pitch angle α (dashed line) and reference angle α_r (solid line) (CEA); b) pitch angle α (dashed line) and reference angle α_r (solid line) (NCEA); c) tracking error of pitch angle α in CEA (dashed line) and NCEA (solid line); d) plunge displacement in CEA (dashed line) and NCEA (solid line); e) control input u in CEA (dashed line) and NCEA (solid line); f) control input u in CEA (dashed line) and NCEA (solid line), initial period; g) estimated parameters for NCEA law [$\|z_1 + \theta_1\|$ (dashed line) and $z_2 + \theta_2$ (solid line)]; h) $\Psi^T z$ for NCEA law.

VI. Conclusions

In this paper, a new adaptive control system based on the immersion and invariance theory was designed for the control of a nonlinear aeroelastic system. This design methodology gave a noncertainty-equivalent adaptive control system, which has a modular structure consisting of a stabilizer (control module) and an estimator. The stability analysis for the control module and the identifier was performed separately using two distinct Lyapunov functions. This allowed flexibility in adjusting the rate of convergence of parameter estimation error independently. Then, using a composite Lyapunov function, it was shown that, in the closed-loop system, all signals were bounded and the pitch angle trajectory tracking error and the plunge displacement asymptotically converged to zero. It was also shown that, unlike the certainty-equivalent adaptive controllers, parameter estimates will remain frozen for all future time, if the estimation error attained zero value at any single instant. Of course, in such a situation, the system will recover the performance of a deterministic controller. Simulation results showed regulation of the pitch angle and plunge displacement to the origin, in spite of large parameter uncertainties. Furthermore, it was observed that the noncertainty-equivalent adaptive control law gives better performance compared to the certainty-equivalent control law.

Appendix: Partial Derivatives and System Parameters

1) Partial Derivatives

$$\mu_1 = \gamma_1 \int^{\dot\alpha} \phi_1 \,\mathrm{d}\lambda = \gamma_1 \left[h, \alpha, \dot h, \frac{\dot\alpha}{2}, \alpha^2, \alpha^3, \alpha^4, \alpha^5 \right]^T \dot\alpha$$

$$\mu_2 = -\gamma_2 \int^{\dot\alpha} v \,\mathrm{d}\lambda = \gamma_2 \int^{\dot\alpha} (\phi_1^T \hat\theta_1 + \phi_1^T \mu_1 + c_1 s - \ddot\alpha_r + \lambda\dot{\tilde\alpha}) \,\mathrm{d}\lambda$$

$$= \gamma_2 \left[h\hat\theta_{11} + \alpha\hat\theta_{12} + \dot h\hat\theta_{13} + \frac{\dot\alpha}{2}\hat\theta_{14} + \alpha^2\hat\theta_{15} + \alpha^3\hat\theta_{16} + \alpha^4\hat\theta_{17} + \alpha^5\hat\theta_{18} \right]\dot\alpha + \gamma_2 \left[c_1 \left(\frac{\dot\alpha^2}{2} - \dot\alpha_r\dot\alpha \right) + c_1\lambda\tilde\alpha\,\dot\alpha - \ddot\alpha_r\dot\alpha + \lambda\left(\frac{\dot\alpha^2}{2} - \dot\alpha_r\dot\alpha \right) \right] + \gamma_2\gamma_1 \left[\{ h^2 + \alpha^2 + \dot h^2 + \alpha^4 + \alpha^6 + \alpha^8 + \alpha^{10} \} \frac{\dot\alpha^2}{2} + \frac{\dot\alpha^4}{8} \right]$$

$$\frac{\partial\mu}{\partial\hat\theta} = \begin{pmatrix} \frac{\partial\mu_1}{\partial\hat\theta} \\ \frac{\partial\mu_2}{\partial\hat\theta} \end{pmatrix} = \begin{pmatrix} 0_{8\times8} & 0_{8\times1} \\ \gamma_2\gamma_1^{-1}\mu_1^T & 0_{1\times1} \end{pmatrix} \in R^{9\times9}$$

$$\frac{\partial\mu_2}{\partial t} = -\gamma_2(c_1\dddot\alpha_r\dot\alpha + \ddot\alpha_r\dot\alpha + \lambda\ddot\alpha_r\dot\alpha + c_1\lambda\dot\alpha_r\dot\alpha), \qquad \frac{\partial\mu_1}{\partial t} = 0_{8\times1}$$

$$\frac{\partial\mu_1}{\partial h} = [\gamma_1\dot\alpha, 0, 0, 0, 0, 0, 0, 0]^T$$

$$\frac{\partial\mu_2}{\partial h} = \gamma_2\hat\theta_{11}\dot\alpha + \gamma_1\gamma_2 h\dot\alpha^2$$

$$\frac{\partial\mu_1}{\partial\alpha} = \gamma_1[0, 1, 0, 0, 2\alpha, 3\alpha^2, 4\alpha^3, 5\alpha^4]^T\dot\alpha$$

$$\frac{\partial\mu_2}{\partial\alpha} = \gamma_2(\hat\theta_{12} + 2\alpha\hat\theta_{15} + 3\alpha^2\hat\theta_{16} + 4\alpha^3\hat\theta_{17} + 5\alpha^4\hat\theta_{18})\dot\alpha + \gamma_2 c_1\lambda\dot\alpha + \gamma_2\gamma_1(2\alpha + 4\alpha^3 + 6\alpha^5 + 8\alpha^7 + 10\alpha^9)\frac{\dot\alpha^2}{2}$$

$$\frac{\partial\mu_1}{\partial\dot h} = [0, 0, \gamma_1\dot\alpha, 0, 0, 0, 0, 0]^T$$

$$\frac{\partial\mu_2}{\partial\dot h} = \gamma_2\hat\theta_{13}\dot\alpha + \gamma_2\gamma_1\dot h\dot\alpha^2 = \gamma_2\dot\alpha(\hat\theta_{13} + \gamma_1\dot h\,\dot\alpha)$$

2) System Parameters

$b = 0.135\,\mathrm{m}$, $m_w = 2.049\,\mathrm{kg}$, $c_h = 27.43\,\mathrm{Ns/m}$, $c_\alpha = 0.036\,\mathrm{Ns}$

$\rho = 1.225\,\mathrm{kg/m^3}$, $c_{l\alpha} = 6.28$, $c_{l\beta} = 3.358$, $c_{m\alpha} = (0.5 + a)c_{l\alpha}$

$c_{m\beta} = -0.635$, $m_t = 12.387\,\mathrm{kg}$, $I_\alpha = 0.0517 + m_w x_\alpha^2 b^2\,\mathrm{kg\cdot m^2}$

$x_\alpha = [0.0873 - (b + ab)]/b$

$k_\alpha = 2.82 \times (1 - 22.1\alpha + 1315.5\alpha^2 - 8580\alpha^3 + 17289.7\alpha^4)\,\mathrm{N\cdot m/rad}$

$k_{h0} = 2844.4\,\mathrm{N/m}$

3) Poles and zeros of linearized model, and θ_i

Case A

Zeros: $-1.6279 \pm 17.5836i$

Poles: $1.1975 \pm 13.0787i$, $-3.3905 \pm 13.5807i$

θ_1: $10^5 * [0.0035, -0.0012, 0.0000, -0.0000, 0.0114 - 0.6803, 4.4371, -8.9412]$

θ_2: 0.0218

Case B

Zeros: $-1.6589 \pm 17.5807i$

Poles: $2.2236 \pm 14.1154i$, $-4.6026 \pm 14.3078i$

θ_1: $10^5 \times [0.0035, -0.0015, -0.0000, -0.0000, 0.0114 - 0.6803, 4.4371, -8.9412]$

θ_2: 0.0139

Case C

Zeros: $-1.9561 \pm 15.3484i$

Poles: $-1.4539 \pm 14.9148i$, 3.0004, -3.5873

θ_1: $10^5 \times [0.0006, 0.0002, 0.0000, -0.0000, 0.0120 - 0.7166, 4.6739, -9.4184]$

θ_2: 0.0159

Case D

Zeros: $-2.1566 \pm 15.3215i$

Poles: 6.6324, -7.3235, $-1.4749 \pm 14.8472i$

θ_1: $10^5 \times [0.0006, 0.0005, 0.0000, -0.0000, 0.0120 - 0.7166, 4.6739, -9.4184]$

θ_2: 0.0102

References

[1] Fung, Y. C., *An Introduction to the Theory of Aeroelasticity*, Wiley, New York, 1955, pp. 207–215.

[2] Dowell, E. H. (ed.), *A Modern Course in Aeroelasticity*, Kluwer Academic, Norwell, MA, 1995, Chap. 1.

[3] Mukhopadhyay, V., "Historical Perspective on Analysis and Control of Aeroelastic Responses," *Journal of Guidance, Control, and Dynamics*, Vol. 26, No. 5, 2003, pp. 673–684. doi:10.2514/2.5108

[4] Lind, R., and Brenner, M., *Robust Aeroservoelastic Stability Analysis*, Springer–Verlag, Berlin, 1999.

[5] Waszak, M. R., "Robust Multivariable Flutter Suppression for the Benchmark Active Control Technology Wind-Tunnel Model," *Journal of Guidance, Control, and Dynamics*, Vol. 24, No. 1, 2001, pp. 147–153. doi:10.2514/2.4694

[6] Scott, R. C., Hoadley, S. T., Wieseman, C. D., and Durham, M. H., "Benchmark Active Controls Technology Model Aerodynamic Data,"

Journal of Guidance, Control, and Dynamics, Vol. 23, No. 5, 2000, pp. 914–921.
doi:10.2514/2.4632

[7] Bennett, R. M., Scott, R. C., and Wieseman, C. D., "Computational Test Cases for the Benchmark Active Controls Model," *Journal of Guidance, Control, and Dynamics*, Vol. 23, No. 5, 2000, pp. 922–929.
doi:10.2514/2.4634

[8] Mukhopadhyay, V., "Transonic Flutter Suppression Control Law Design and Wind-Tunnel Test Results," *Journal of Guidance, Control, and Dynamics*, Vol. 23, No. 5, 2000, pp. 930–937.
doi:10.2514/2.4635

[9] Kelkar, A. G. and Joshi, S. M., "Passivity-Based Robust Control with Application to Benchmark Active Controls Technology Wing," *Journal of Guidance, Control, and Dynamics*, Vol. 23, No. 5, 2000, pp. 938–947.
doi:10.2514/2.4636

[10] Barker, J. M., and Balas, G. J., "Comparing Linear Parameter-Varying Gain-Scheduled Control Techniques for Active Flutter Suppression," *Journal of Guidance, Control, and Dynamics*, Vol. 23, No. 5, 2000, pp. 948–955.
doi:10.2514/2.4637

[11] Guillot, D. M., and Friedmann, P. P., "Fundamental Aeroservoelastic Study Combining Unsteady Computational Fluid Mechanics with Adaptive Control," *Journal of Guidance, Control, and Dynamics*, Vol. 23, No. 6, 2000, pp. 1117–1126.
doi:10.2514/2.4663

[12] Scott, R. C., and Pado, L. E., "Active Control of Wind-Tunnel Model Aeroelastic Response Using Neural Networks," *Journal of Guidance, Control, and Dynamics*, Vol. 23, No. 6, 2000, pp. 1100–1108.
doi:10.2514/2.4661

[13] Ko, J., Kurdila, A. J., and Strganac, T. W., "Nonlinear Control of a Prototypical Wing Section with Torsional Nonlinearity," *Journal of Guidance, Control, and Dynamics*, Vol. 20, No. 6, 1997, pp. 1181–1189.
doi:10.2514/2.4174

[14] Ko, J., Strganac, T. W., and Kurdila, A. J., "Stability and Control of a Structurally Nonlinear Aeroelastic System," *Journal of Guidance, Control, and Dynamics*, Vol. 21, No. 5, 1998, pp. 718–725.
doi:10.2514/2.4317

[15] Block, J. J., and Strganac, T. W., "Applied Active Control for a Nonlinear Aeroelastic Structure," *Journal of Guidance, Control, and Dynamics*, Vol. 21, No. 6, 1998, pp. 838–845.
doi:10.2514/2.4346

[16] Lee, K. W., and Singh, S. N., "Global Robust Control of an Aeroelastic System Using Output Feedback," *Journal of Guidance, Control, and Dynamics*, Vol. 30, No. 1, 2007, pp. 271–275.
doi:10.2514/1.22940

[17] Xing, W., and Singh, S. N., "Adaptive Output Feedback Control of a Nonlinear Aeroelastic Structure," *Journal of Guidance, Control, and Dynamics*, Vol. 23, No. 6, 2000, pp. 1109–1116.
doi:10.2514/2.4662

[18] Ko, J., Strganac, T. W., and Kurdila, A. J., "Adaptive Feedback Linearization for the Control of a Typical Wing Section with Structural Nonlinearity," *Nonlinear Dynamics*, Vol. 18, No. 3, 1999, pp. 289–301.
doi:10.1023/A:1008323629064

[19] Behal, A., Rao, V. M., Marzocca, P., and Kamaludeen, M., "Adaptive Control for a Nonlinear Wing Section with Multiple Flaps," *Journal of Guidance, Control, and Dynamics*, Vol. 29, No. 3, 2006, pp. 744–749.
doi:10.2514/1.18182

[20] Singh, S. N., and Brenner, M., "Modular Adaptive Control of a Nonlinear Aeroelastic System," *Journal of Guidance, Control, and Dynamics*, Vol. 26, No. 3, 2003, pp. 443–451.
doi:10.2514/2.5082

[21] Astofi, A., and Ortega, R., "Immersion and Invariance: A New Tool for Stabilization and Adaptive Control of Nonlinear Systems," *IEEE Transactions on Automatic Control*, Vol. 48, No. 4, 2003, pp. 590–606.
doi:10.1109/TAC.2003.809820

[22] Karagiannis, D., and Astolfi, A., "Nonlinear Adaptive Control of Systems in Feedback Form: An Alternative to Adaptive Backstepping," *IFAC Symposium on Large Scale Systems: Theory and Applications*, Elsevier, Amsterdam, 2004, pp. 67–72.

[23] Astolfi, A., Karagiannis, D., and Ortega, R., *Nonliear and Adaptive Control with Applications*, Springer–Verlag, London, 2008, pp. 276–309.

[24] Seo, D., and Akella, M. R., "High-Performance Spacecraft Attitude-Tracking Control Through Attracting-Manifold Design," *Journal of Guidance, Control, and Dynamics*, Vol. 31, No. 4, 2008, pp. 884–891.
doi:10.2514/1.33308

[25] Singh, S. N., and Brenner, M., "Limit Cycle Oscillation and Orbital Stability in Aeroelastic Systems with Torsional Nonlinearity," *Nonlinear Dynamics*, Vol. 31, No. 4, 2003, pp. 435–450.
doi:10.1023/A:1023264319167